Bioactive Materials 2 (2017) 253–259

Contents lists available at ScienceDirect

Bioactive Materials

journal homepage: http://www.keaipublishing.com/en/journals/bioactive-materials/

In situ assembly of fibrinogen/hyaluronic acid hydrogel via knob-hole interaction for 3D cellular engineering

Shengjie Huang, Chunfen Wang, Jingwei Xu, Lie Ma*, Changyou Gao

MOE Key Laboratory of Macromolecular Synthesis and Functionalization, Department of Polymer Science and Engineering, Zhejiang University, Hangzhou, 310027, China

ARTICLE INFO

Article history:
Received 1 September 2017
Received in revised form
14 September 2017
Accepted 15 September 2017
Available online 21 September 2017

Keywords:
Fibrinogen
Knob-hole interactions
Hyaluronic acid
In situ assembly
Cell encapsulation

ABSTRACT

Hyaluronic acid (HA)-based hydrogels have applied widely for biomedical applications due to its biocompatibility and biodegradability. However, the use of initiators or crosslinkers during the hydrogel formation may cause cytotoxicity and thereby impair the biocompatibility. Inspired by the crosslinking mechanism of fibrin gel, a novel HA-based hydrogel was developed via the *in situ* supramolecular assembly based on knob-hole interactions between fibrinogen and knob-grafted HA (knob-g-HA) in this study. The knob-grafted HA was synthesized by coupling knob peptides (GPRPAAC, a mimic peptide of fibrin knob A) to HA via Michael addition. Then the translucent fibrinogen/knob-g-HA hydrogels were prepared by simply mixing the solutions of knob-g-HA and fibrinogen at the knob/hole ratio of 1.2. The rheological behaviors of the fibrinogen/knob-g-HA hydrogels with the fibrinogen concentrations of 50, 100 and 200 mg/mL were evaluated, and it was found that the dynamic storage moduli (G′) were higher than the loss moduli (G″) over the whole frequency range for all the groups. The SEM results showed that fibrinogen/knob-g-HA hydrogels presented the heterogeneous mesh-like structures which were different from the honeycomb-like structures of fibrinogen/MA-HA hydrogels. Correspondingly, a higher swelling ratio was obtained in the groups of fibrinogen/knob-g-HA hydrogel. Finally, the cytocompatibility of fibrinogen/knob-g-HA hydrogels was proved by live/dead stainings and MTT assays in the 293T cells encapsulation test. All these results highlight the biological potential of the fibrinogen/knob-g-HA hydrogels for 3D cellular engineering.

1. Introduction

With the exquisite nano- and micro-scale features of extracellular matrix (ECM), hydrogels have become a class of biomaterials for cell encapsulation, tissue engineering and regenerative medicine in recent years. Currently, hydrogels fabricated from the natural materials including collagen, hyaluronic acid (HA), and alginate are attracted much attention. Among them, HA, which is abundant in many tissues of the body [1], plays vital roles in cellular behaviors and physiological processes such as proliferation [2,3] morphogenesis [4,5] migration [6] inflammation and wound healing [7–9]. HA has been used widely in the fields of surface coating, drug/gene delivery [10], and particularly tissue engineering [11]. The biocompatibility and biodegradability make HA hydrogel to be an attractive matrix for regenerating a wide variety of tissues and organs such as cartilage [12,13], adipose [14,15], brain [16,17], and blood vessel [18].

To obtain the robust mechanical property, HA hydrogels are normally formed by a covalent crosslinking by the addition of crosslinkers, catalysts or photoinitiators, which may cause cytotoxicity [19–23]. Currently, several strategies were reported to avoid these disadvantages. For example, HA hydrogels were crosslinked via Diels-Alder reaction to avoid impairing the biocompatibility [24]. In our previous work, Xing et al. prepared a bioactive HA-based hydrogel by Diels-Alder reaction between the CQAASIKVAV peptide-modified furan-HA and the bismaleimide-functionalized poly(ethylene glycol) (PEG) for promoting neurite outgrowth of PC12 cells [25]. Crescenzi et al. also developed a novel crosslinking procedure based on copper-catalyzed azide-alkyne cycloaddition to form the HA-based gels *in situ*, which did not show toxic for both yeast cells and red blood cells [26]. Recently, Broguiere et al. demonstrated the specific transglutaminase activity of the activated blood coagulation factor XIII (FXIIIa) on accelerating

* Corresponding author.
E-mail address: liema@zju.edu.cn (L. Ma).
Peer review under responsibility of KeAi Communications Co., Ltd.

http://dx.doi.org/10.1016/j.bioactmat.2017.09.002

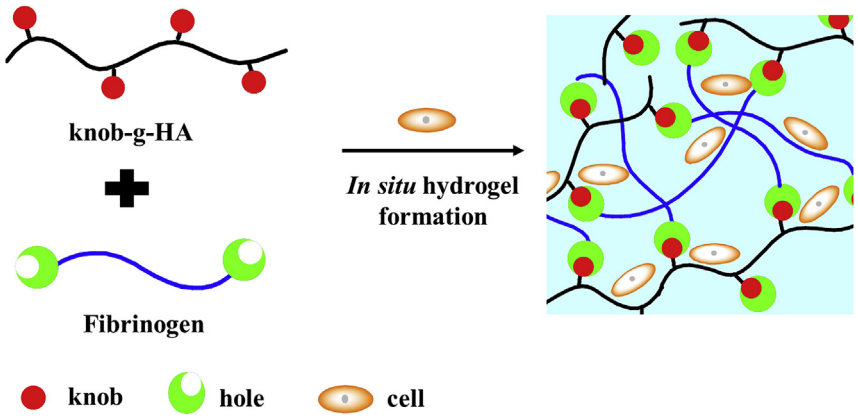

Scheme 1. Schematic illustration of the formation of fibrinogen/hyaluronic acid hydrogel via knob-hole interaction for cells encapsulation.

the reaction between lysine and glutamine of HA derivatives, and thus the formation of HA hydrogels [27].

Supramolecular assembly, based on natural host-guest pairs such as biotin and avidin or synthetic pairs like cyclodextrin and PEG, has been employed in the fields of surface modifications [28], molecular separation [29], drug delivery and hydrogels formation [30,31]. Park et al. prepared a supramolecular hydrogel of cucurbit [6]uril (CB[6])-conjugated HA via the interaction between CB[6] and diaminohexane (DAH). The CB[6]/DAH-HA hydrogels were feasible to deliver proper cues for cellular proliferation and differentiation [32]. Thompson et al. reported a series of noncovalent hydrogels crosslinked by receptor-ligand interactions between biotinylated PEG and avidin. Furthermore, the hydrogels based RGD- and metal matrix proteinase (MMP)-functionalized biotinylated PEGs were proved to be biocompatible with the improved spreading of mesenchymal stem cells (MSCs) [33].

As one of the main components in plasma [34], fibrinogen avoids eliciting an inflammatory response, foreign body reaction and other adverse reactions and has been an attractive material for regenerative medicine. With the development of molecular biology, the molecular mechanism of the conversion of fibrinogen into fibrin was disclosed gradually [35,36]. Fibrinogen is a 45 nm long and 340 kD large glycoprotein consisting of three pairs of polypeptide chains (Aα, Bβ, and γ) [37,38]. Cleaved by thrombin, a pair of binding sites (knob A/B) was generated at the fibrinopeptide A (FpA) and B (FpB) in the central N-terminal part of E-domain. Under a specific interaction between “knob” and “hole” (the site in the D-domains of fibrinogen), the fibrin fibers are aggregated and further covalently crosslinked into stable clots by FXIIIa. It was found that the yield force between “knob” and “hole” is comparable with the strongest noncovalent interaction between streptavidin and biotin [35]. It gives the potentials to use “knob”-“hole” interaction for engineering a hydrogel.

Inspired by the crosslinking mechanism of fibrin gel, a novel HA-based hydrogel with no decaying in biocompatibility was developed via the “knob”-“hole” interactions between fibrinogen and the knob-grafted HA (knob-g-HA) in this study (Scheme 1). Briefly, knob-g-HA was synthesized by coupling GPRPAAC peptides (knob) to methacrylated HA (MA-HA) via Michael addition reaction. Then the fibrinogen/knob-g-HA hydrogels were prepared by mixing fibrinogen and knob-g-HA solutions. The influences of the fibrinogen concentration and the “knob”/“hole” ratio on gel formation were investigated. The rheological behaviors, swelling properties, and microstructures were also studied. Finally, the application of the fibrinogen/knob-g-HA hydrogels for cells encapsulation was investigated.

2. Material and method

2.1. Materials

Hyaluronic acid (HA, Mw 1.1 × 10^5 Da) was purchased from Zhenjiang Dong Yuan Biotech Co., Ltd. Methacrylic anhydride was bought from Alfa Aesar (Tianjin) chemical Co., Ltd. Cysteine terminating fibrin knob peptide GPRPAAC (knob A) was synthesized by Sangon Biotech (Shanghai) Co., Ltd. Triethanolamine (TEA) was purchased from Sinopharm Chemical Reagent Co., Ltd. 5, 5′-Dithio bis-(2-nitrobenzoic acid) (DTNB) was the product of Aladdin Chemistry Co., Ltd. Human fibrinogen was purchased from Green Cross (China) Bio-products Co., Ltd. Tris(hydroxymethyl)aminomethane (Tris) was obtained from Amresco. Propidium iodide (PI) and 3-(4,5)-dimethylthiazol-2-yl)-2,5-diphenyl tetrazolium bromide (MTT) were purchased from Sigma Chemical Co. Calcein AM(Ca-AM) was purchased from US Everbright Inc., and 2-hydroxy-4’-(2-hydroxyethoxy)-2-methylpropiophenone (2959) was obtained from Tokyo Chemical industry Co., Ltd. All other reagents were analytical grade and used without further treatment if not specially mentioned. Water used in the experiments was purified by Milli-Q water system (Millipore, USA).

2.2. Synthesis of methacrylated HA (MA-HA)

HA was methacrylated according to the method reported previously [39]. Briefly, HA sodium salt (1 g) was dissolved in Milli-Q water (100 mL) at 4 °C under agitation overnight, into which five-fold methacrylic anhydride was added dropwise. The pH value was maintained between 8 and 10 by adding 5 M NaOH. The reaction was carried out in ice bath for 24 h under agitation. Then, NaCl was added to the mixture to a concentration of 0.5 M. MA-HA was collected by precipitating the solution in 5-fold volume of ethanol twice. MA-HA was then dialyzed (MWCO 3500 Da) against deionized water for 4 days, and the final product was obtained by lyophilization and stored at 4 °C. The purified MA-HA was characterized by ^{1}H NMR, from which the methacrylation degree of MA-HA was quantified.

2.3. Synthesis of knob-g-HA

Knob-g-HA was synthesized via Michael addition reaction between the methacrylate groups of MA-HA and the thiol groups of knob peptide. In brief, MA-HA (450 mg) was dissolved in Milli-Q water (15 mL) at room temperature. After complete dissolution, 30 mL nucleophilic buffering reagent TEA (30 mM) was added to

obtain the MA-HA/TEA buffer solution. Under the atmosphere of nitrogen, knob A (90 mg) was added, and the solution was incubated for 24 h at room temperature with gentle agitation. At predetermined time points, 40 μL reacting solution was removed and diluted into 160 μL Tris buffer solution. Then 0.1 mM DTNB solution was added to trace the reaction processes. To purify knob-g-HA, the reaction solution was added into 250 mL ethanol with vigorous stirring, and the precipitated product was washed twice with ethanol. The knob-g-HA solution underwent four-day dialysis (MWCO 3500 Da) against deionized water, and the lyophilized knob-g-HA was stored at 4 °C until use. ^{1}H NMR analysis was performed to quantify the peptide grafting ratio.

2.4. Preparation of fibrinogen/knob-g-HA hydrogels

A certain amount of knob-g-HA were dissolved into Tris-Ca buffer solution (140 mM NaCl, 5 mM $CaCl_2$, 20 mM Tris, pH 7.4) to prepare the knob-g-HA solution. Then the equal volume of fibrinogen solution (200 mg/mL) were mixed with the knob-g-HA solution to yield the fibrinogen/knob-g-HA hydrogel, noted as F(200)/knob-g-HA. To determine the effect of the knob: hole ratio on hydrogel formation, a series of hydrogels with the knob: hole mole ratios of 0.5:1, 1:1, 1.2:1, 1.5:1, 2:1, and 10:1 were prepared, respectively. The formation of hydrogel was determined by the tube inverting method. Changing knob-g-HA to MA-HA, Fibrinogen/MA-HA hydrogels were also prepared according to the similar procedure with fibrinogen solution of 200 mg/mL and treated under ultraviolet irradiation(365 nm, 1.2 mW/cm^2) for 3min with addition of photoinitiator 2959 (0.2% w/v).

2.5. Rheological measurement

Rheological analysis was performed by an ARG2 rheometer (TA Instruments Inc.) with standard steel parallel-plate geometry (20 mm diameter). The knob-g-HA solutions and fibrinogen solutions were mixed with different fibrinogen concentrations, and then the mixed solutions were injected onto the plate. The rheological tests were performed 5 mins later for complete gelation. To ensure the measurements were performed in the linear viscoelastic region, the dynamic strain sweep tests were performed on the hydrogels at a 1.0 Hz oscillation frequency to discover the linear viscoelastic region. The dynamic storage (G′) and loss (G″) moduli were monitored at a constant strain amplitude (0.1%) as a function of frequency.

2.6. Microstructure observation

The hydrogel samples for microstructure observation were prepared by being immersed into liquid nitrogen for 15 min and freeze-dried overnight. Then,the cross-sectional surface of the samples were coated with gold and examined by a scanning electron microscopy (SEM S-3000N, Hitachi, Japan) with an accelerating voltage of 3.0 kV.

2.7. Swelling ratio measurement

Briefly, the fibrinogen/knob-g-HA hydrogels were lyophilized and weighed (W_0). Then, the dried samples were immersed in 2 mL of PBS (pH 7.4) at 37 °C. At each interval, after removed the surface water by a filter paper, the samples were weighed again (W_t). The swelling ratios were calculated by the formula of $(W_t\text{-}W_0)/W_0 \times 100\%$.

2.8. Cell encapsulation test

The biocompatibility of the fibrinogen/knob-g-HA hydrogel was evaluated by the encapsulation test of 293T cells, taking the fibrinogen/MA-HA hydrogel as control. Briefly, 293T cells were suspended in the fibrinogen solution at a density of 3×10^6 cells/mL. The cells suspension (200 μL) was then mixed with the same volume of knob-g-HA directly or MA-HA solution with 0.4% photoinitiator 2959. After gel formation, 200 μL high-glucose DMEM (Gibco, USA) supplemented with 10% fetal bovine serum (FBS, Sijiqing Inc., Hangzhou, China), 100 U/mL penicillin and 100 g/mL streptomycin was added. Then, the cell-laden hydrogels were cultured at 37 °C under 5% CO_2.

Live/dead staining and MTT assay were applied to investigate the viability of the encapsulated 293T cells. The samples of after encapsulation immediately and after 1 day and 3 days culture were incubated in the solution of Ca-AM (2 μg/mL) and PI (10 μg/mL) for 30 min at 37 °C. After washed with PBS (pH 7.4) for 3 times, the cell morphologies were observed under a fluorescence microscope (X-Cite Series 120Q, Canada). For MTT assay, at each interval, the culture medium was aspirated and then the samples were washed twice with PBS (pH 7.4). Then, 100 μL MTT solution (0.5 mg/mL) was added to each sample and further incubated for 4 h at 37 °C. After removed the medium, 500 μL dimethyl sulphoxide (DMSO) was added to dissolve the formazan crystals. After centrifugation of the resulting solution at 5000 rpm for 10 min, 200 μL supernatant was pipetted and placed in a 96-well plate. The optical density of the solution was recorded using a Microplate Reader (Bio-Rad, model 680, USA) at a wavelength of 570 nm.

2.9. Statistical analysis

The swelling experiments and MTT assays were performed with at least three samples, respectively. Experimental data were expressed as mean ± standard deviation (SD) and the significant difference were analyzed by one way of variance (ANOVA) by using SPSS software (SPSS Inc., Chicago, USA). The significant level was set as $p < 0.05$.

3. Results and discussion

3.1. Synthesis and characterization of knob-g-HA

HA was modified by methacrylic anhydride via esterification reaction to obtain methacrylated HA (MA-HA), to which knob was then grafted via Michael addition reaction to yield knob-g-HA as schematically shown in Fig. 1 A. As shown in the ^{1}H NMR spectra in Fig. 1 B, the unmodified HA showed several typical peaks at δ4.42, 4.33, 3.1–3.8 and 1.89 ppm. For MA-HA, two peaks at δ 6.05 and 5.62 ppm, as well as peaks near 1.89 ppm could be assigned to -CH_2 and -CH_3 of methacrylate groups, respectively. Taking the methyl resonance of MA-HA at δ 1.56–1.95 ppm as an internal standard, the degree of methacrylate modification was calculated as ~37.88%. Compared to MA-HA, the spectra of knob-g-HA showed that the signal at δ 6.05 and 5.62 ppm decreased and the peaks at 3.34 ppm ($H_2N\text{-}CH_2\text{-}CO$-, G), 2.90 and 2.72 ppm (-CH-CH_2-S-, C), 2.20 ppm (-CH-CH_2-CH_2-, P), 1.29 ppm (-CH-CH_2-CH_2, R), and 1.11 ppm (-HN-CH(CH_3)-CO-, A) could be assigned to the amino acids of knob peptide (GPRPAAC). These results demonstrated the successful synthesis of knob-g-HA. Furthermore, determined by the decrease of the signal at δ 6.05 and 5.62 ppm, the knob-grafting ratio was calculated as 18.7%.

3.2. Formation of fibrinogen/knob-g-HA hydrogels

To investigate the effect of the “knob”/“hole” ratio on hydrogel formation, an equal volume of fibrinogen and knob-g-HA with varied concentration were mixed. As shown in Fig. 2 A, a

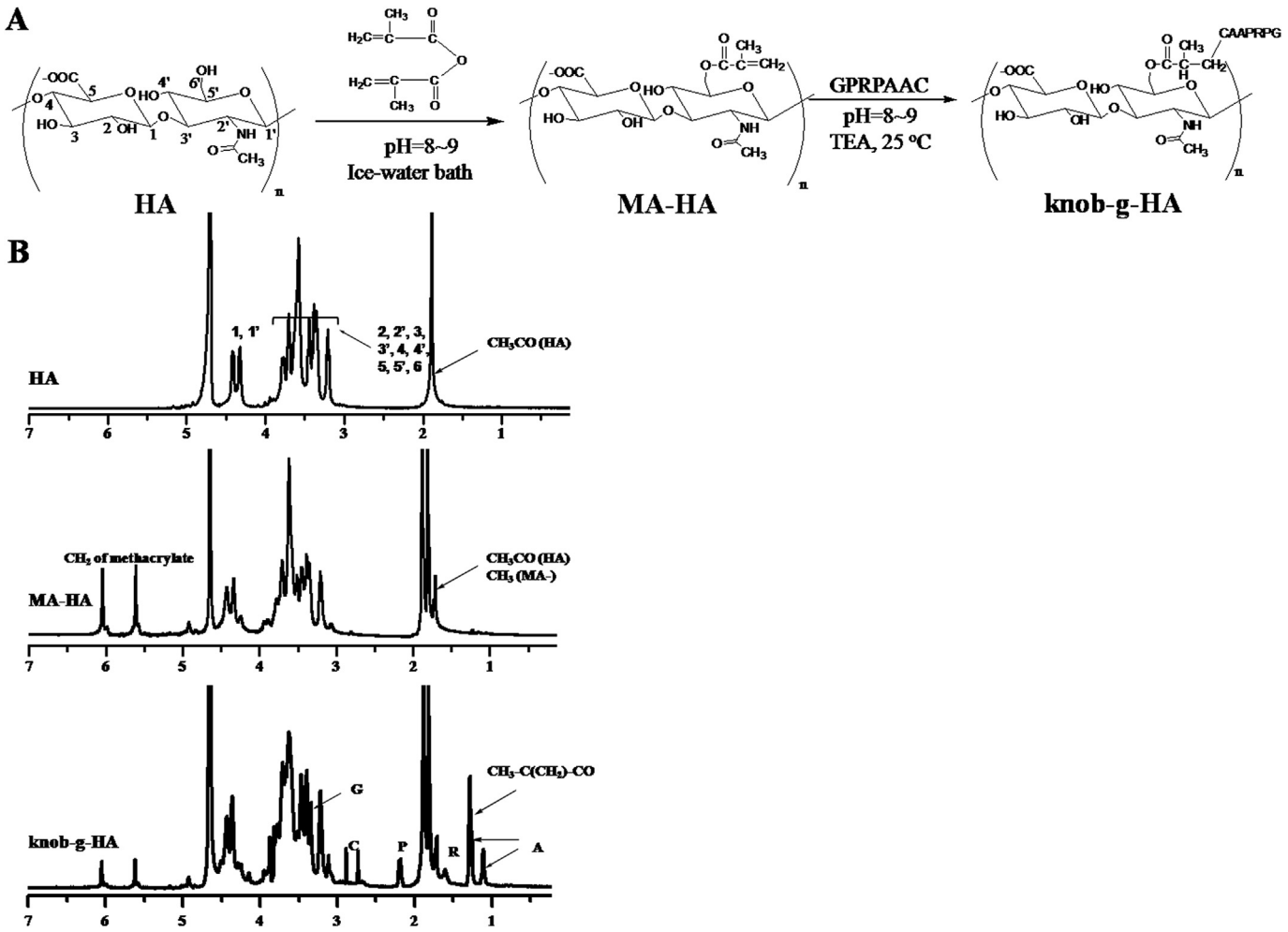

Fig. 1. Synthesis route (A) and ^{1}H NMR spectra (B) of knob-g-HA.

translucent hydrogel was formed only when the ratio is 1.2, and no stable hydrogel could be formed when the ratios are lower or higher than this value. In theory, a cross-linked network should be generated when the "knob"/"hole" ratio of equals to 1. However, because of the entanglement and steric hindrance between knob-g-HA macromolecules, it is hard for "knob" to engage fully with "hole". Therefore, a higher "knob"/"hole" ratio was needed. However, the further increase of the ratio would result in a lower crosslinking efficiency of fibrinogen, which has two holes at the end of each molecule. Furthermore, the effect of the fibrinogen concentration on the hydrogel formation was also investigated. It was found that the mixtures became more solid when the fibrinogen concentration increased from 50 to 200 mg/mL.

3.3. Rheological properties

The rheological behaviors of the fibrinogen/knob-g-HA hydrogels with the fibrinogen concentrations of 50, 100 and 200 mg/mL (named as F(50)/knob-g-HA, F(100)/knob-g-HA and F(200)/knob-g-HA, respectively) were evaluated and presented in Fig. 2 B. It showed that the storage modulus (G′) for all the hydrogels were higher than the corresponding loss modulus (G″) over the full frequency range, indicating the formation of the fibrinogen/knob-g-HA hydrogels. With the increase of the fibrinogen concentrations, the higher G′ and G″ of the hydrogels were obtained, indicating the increased mechanical strength and the shape retention property. When the "knob"/"hole" ratio fixed, the crosslinking density of the hydrogels increased with the augment of the fibrinogen concentrations. In general, the mechanical strength of the fibrinogen/knob-g-HA hydrogel is relatively weak. Although the knob-hole interaction has a very high binding constant similar to that of biotin-streptavidin interaction, the mechanical property of knob-g-HA/Fibrinogen gel is also determined by many other factors such as the cross-linking density. As fibrinogen is a 45 nm long and 340 kD large molecule with only two holes in distal C-terminal [36], the binding sites might be encapsulated inside the huge biomolecule, and therefore the reaction probability of with holes would be reduced, resulting in a low cross-linking density and low mechanical properties. However, at a fibrinogen concentration of 200 mg/mL, the fibrinogen/knob-g-HA hydrogel was robust enough to hold its shape (data not shown) and support cell culture. It is hard to prepare a more robust hydrogel by the further increase of fibrinogen concentration as the fibrinogen solution is too viscous to be operated when it is higher than 200 mg/mL.

3.4. Microstructures and swelling behaviors

The microstructures of the fibrinogen/knob-g-HA hydrogels with different fibrinogen concentrations and the fibrinogen/MA-HA hydrogels were presented in Fig. 3 A. The heterogeneous mesh-like structures were observed in the groups of fibrinogen/knob-g-HA hydrogels (Fig. 3 A: a, b, c, e, f, g). For F (50)/knob-g-

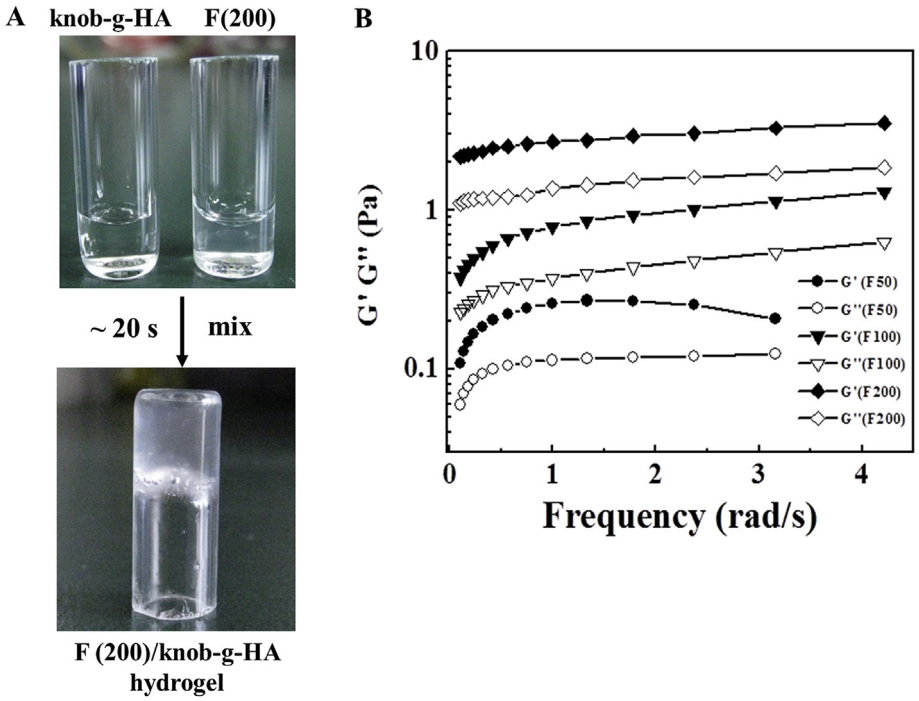

Fig. 2. (A) Photographs of the forming process of the fibrinogen/knob-g-HA hydrogel with a fibrinogen concentration of 200 mg/mL. (B) Frequency sweep rheological analysis for storage (G′) and loss (G″) moduli of the fibrinogen/knob-g-HA hydrogels with different fibrinogen concentrations.

HA hydrogels, the porous structures on the surface were collapsed a little (Fig. 3 A: a, e). While, with the increase of the fibrinogen concentration, the porous structures were kept better. Besides the fiber structures, more sheet-like structures were presented with the bigger pore sizes (Fig. 3 A: b, c, f, g). These results are contributed to the increasing crosslinking densities with the increasing fibrinogen concentrations, which are consistent with the results of rheological measurements. In contrast, the fibrinogen/MA-HA hydrogels showed honeycomb-like structures with dense sheet-like walls, which were significantly different from that of the fibrinogen/MA-HA hydrogels (Fig. 3 A: d, h). It is known that the crosslinking of the fibrinogen/MA-HA hydrogels was based on the

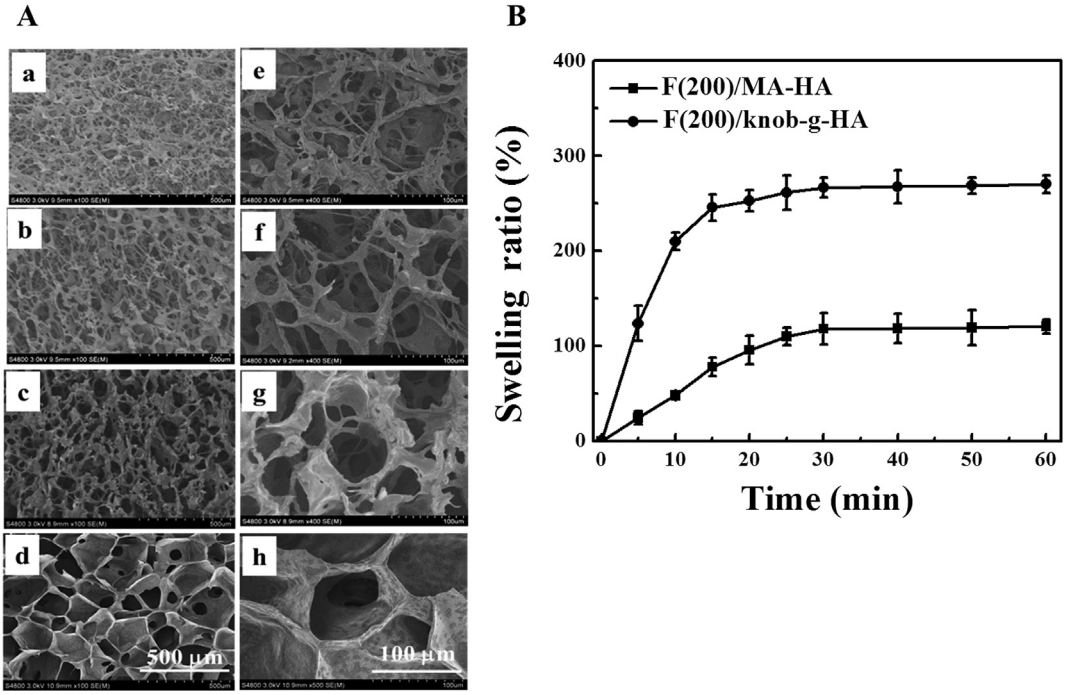

Fig. 3. (A) SEM images of the fibrinogen/knob-g-HA hydrogels with the fibrinogen concentrations of 50 mg/mL (a), 100 mg/mL (b), and 200 mg/ml(c). (d) is the fibrinogen/MA-HA hydrogel with a concentration of 200mg/mL. (e–h) are the corresponding images with higher magnification. (B) Swelling ratios of F(200)/knob-g-HA and F(200)/MA-HA hydrogels.

free radical polymerization of MA-HA with the addition of the photoinitiator 2959 and under UV irradiation, which resulted in much higher crosslinking densities and thereby the denser networks. However, for the fibrinogen/knob-g-HA hydrogels, because of the relatively longer distance between the crosslinking points, the looser mesh-like structures were formed inside the hydrogels. Such porous and interconnected structures can provide efficient channels for rapid transport of water, nutrients, and metabolites, which is beneficial for cell growth.

Fig. 3 B showed the swelling ratios of the hydrogels in PBS (pH 7.4) with the immersion time. It was remarkable to note that the fibrinogen/knob-g-HA hydrogels exhibited higher swelling ratios than the fibrinogen/MA-HA hydrogels. The swelling ratios of the fibrinogen/knob-g-HA hydrogel increased rapidly. It just took 15 min to reach swelling equilibrium, resulting in a swelling ratio of ~270%. As to the fibrinogen/MA-HA hydrogels, the time to reach equilibrium swelling (with a ratio of 120%) is about 30 min. It could be explained by the microstructure difference as explored by SEM. The interconnected mesh-like structures of the fibrinogen/knob-g-HA hydrogels were more conducive for substance exchange than the honeycomb-like structures of the fibrinogen/MA-HA hydrogels.

3.5. Cytocompatibility

The cytotoxicities of the fibrinogen/knob-g-HA and fibrinogen/MA-HA hydrogels were compared using a live/dead cell staining. As presented in Fig. 4 A, the cells could be distributed evenly after encapsulated into both kinds of hydrogels. For the cells encapsulated into the fibrinogen/knob-g-HA hydrogels instantly (0 day), all of them showed green colour, indicating the live state (Fig. 4 A: a).

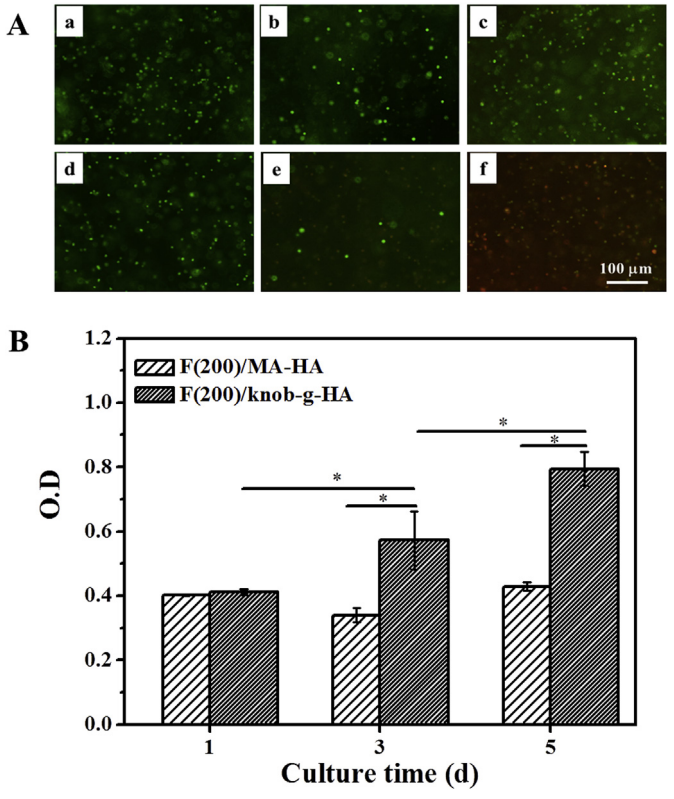

Fig. 4. (A) Live (green)/dead (red) stainings of 293T cells encapsulated in F(200)/Knob-g-HA hydrogels (a-c) and F(200)/MA-HA hydrogels (d–f) for 0 day (a, d), 1 day (b, e) and 3 days (c, f), respectively. (B) Cell viabilities of 293T cells in F(200)/knob-g-HA hydrogels and F(200)/MA-HA hydrogels for different time.

When the culture time increased to 1 day, there was still no cell in red colour (Fig. 4 A: b). After incubation for 3 days, only a few of cells were stained by red, and above 90% cells were alive (Fig. 4 A: c). While, for the case of the fibrinogen/MA-HA hydrogels, many red cells could be observed after 1 day culture. Few of cells showed green after incubated for 3 days, indicating the cells were almost dead (Fig. 4 A: c).

The viabilities of the cells in both hydrogels were also evaluated by MTT assay (Fig. 4 B). For the fibrinogen/MA-HA group, the viabilities did not increase with the prolongation of culture time. On the contrary, the cell viabilities of the fibrinogen/knob-g-HA group increased with the culture time. Furthermore, except for the samples of day 1, much higher cell viabilities in the fibrinogen/knob-g-HA group were detected than those of the fibrinogen/MA-HA group at the other time intervals, indicating the better cytocompatibility to support cell proliferation. These differences could be attributed to the cytotoxicity of photo initiators and UV irradiations during the preparation of the fibrinogen/MA-HA hydrogels, which has been reported in many previous studies [27,40,41]. In summary, the *in situ* formation of fibrinogen/knob-g-HA hydrogels base on “knob”-“hole” interaction shows the unique characteristics for the applications for 3D cellular engineering.

4. Conclusions

The fibrinogen/knob-g-HA hydrogels based on the “knob” - “hole” interaction were facilely fabricated. It was found that when the “knob”/“hole” ratio is 1.2, a translucent hydrogel was formed. Higher storage moduli were detected with the increase of the fibrinogen concentrations, indicating the more robust hydrogels were obtained. Compared to the honeycomb-like structures of the fibrinogen/MA-HA hydrogels, the heterogeneous mesh-like structures were observed in the fibrinogen/knob-g-HA hydrogels, which exhibited higher swelling ratios correspondingly. It was further shown that the cells encapsulated in the fibrinogen/knob-g-HA hydrogels had a higher viability than that in the fibrinogen/MA-HA hydrogels. All the results demonstrated that the supramolecular assembly via “knob”-“hole” interactions would be a facile method to prepare a HA-based hydrogel with good biocompatibility, which is suitable for various biomedical applications such as tissue engineering and regenerative medicine.

Acknowledgements

The authors acknowledge the financial support by the National Natural Science Foundation of China (51673167 and 21434006), the National Key Research Program of China (2017YFA0104901) and the Fundamental Research Funds for the Central Universities (2017XZZX008-05).

References

[1] E. Hachet, H. Van den Berghe, E. Bayma, M.R. Block, R. Auzély-Velty, Design of biomimetic cell-interactive substrates using hyaluronic acid hydrogels with tunable mechanical properties, Biomacromolecules 13 (2012) 1818–1827.
[2] M. Inoue, C. Katakami, The effect of hyaluronic acid on corneal epithelial cell proliferation, Investig. Ophth. Vis. Sci. 34 (1993) 2313–2315.
[3] Y. Lei, S. Gojgini, J. Lam, T. Segura, The spreading, migration and proliferation of mouse mesenchymal stem cells cultured inside hyaluronic acid hydrogels, Biomaterials 32 (2011) 39–47.
[4] B.P. Toole, Hyaluronan in morphogenesis, Semin. Cell Dev. Biol. 12 (2001) 79–87.
[5] B.P. Toole, Hyaluronan: from extracellular glue to pericellular cue, Nat. Rev. Cancer 4 (2004) 528–539.
[6] E. Anitua, M. Sanchez, M.D.L. Fuente, M.M. Zalduendo, G. Orive, Plasma rich in growth factors (PRGF-Endoret) stimulates tendon and synovial fibroblasts migration and improves the biological properties of hyaluronic acid, Knee Surg. Sport. Tr. A 20 (2012) 1657–1665.
[7] P. Weigel, S. Frost, C. McGary, R. LeBoeuf, The role of hyaluronic acid in

inflammation and wound healing, Int. J. Tissue React. 10 (1987) 355–365.
[8] O.N. Uchakina, C.M. Castillejo, C.C. Bridges, R.J. McKallip, The role of hyaluronic acid in SEB-induced acute lung inflammation, Clin. Immunol. 146 (2013) 56–69.
[9] B.M. Teh, Y. Shen, P.L. Friedland, M.D. Atlas, R.J. Marano, A review on the use of hyaluronic acid in tympanic membrane wound healing, Expert Opin. Biol. Th. 12 (2012) 23–36.
[10] H. Knopf-Marques, et al., Hyaluronic acid and its derivatives in coating and delivery systems: applications in tissue engineering, regenerative medicine and immunomodulation, Adv. Healthc. Mater. 5 (2016) 2841–2855.
[11] J. Lam, N.F. Truong, T. Segura, Design of cell–matrix interactions in hyaluronic acid hydrogel scaffolds, Acta Biomater. 10 (2014) 1571–1580.
[12] H.S. Yoo, E.A. Lee, J.J. Yoon, T.G. Park, Hyaluronic acid modified biodegradable scaffolds for cartilage tissue engineering, Biomaterials 26 (2005) 1925–1933.
[13] I.L. Kim, R.L. Mauck, J.A. Burdick, Hydrogel design for cartilage tissue engineering: a case study with hyaluronic acid, Biomaterials 32 (2011) 8771–8782.
[14] H. Tan, et al., Thermosensitive injectable hyaluronic acid hydrogel for adipose tissue engineering, Biomaterials 30 (2009) 6844–6853.
[15] A. Borzacchiello, et al., Structural and rheological characterization of hyaluronic acid-based scaffolds for adipose tissue engineering, Biomaterials 28 (2007) 4399–4408.
[16] F. Cui, W. Tian, S. Hou, Q. Xu, I.-S. Lee, Hyaluronic acid hydrogel immobilized with RGD peptides for brain tissue engineering, J. Mater. Sci. Mater. M 17 (2006) 1393–1401.
[17] S. Hou, et al., The repair of brain lesion by implantation of hyaluronic acid hydrogels modified with laminin, J. Neurosci. Meth. 148 (2005) 60–70.
[18] A. Remuzzi, et al., Vascular smooth muscle cells on hyaluronic acid: culture and mechanical characterization of an engineered vascular construct, Tissue Eng. 10 (2004) 699–710.
[19] E. Tous, et al., Influence of injectable hyaluronic acid hydrogel degradation behavior on infarction-induced ventricular remodeling, Biomacromolecules 12 (2011) 4127–4135.
[20] N.E. Fedorovich, et al., The effect of photopolymerization on stem cells embedded in hydrogels, Biomaterials 30 (2009) 344.
[21] H. Kim, et al., Hyaluronate and its derivatives for customized biomedical applications, Biomaterials 123 (2017) 155–171.
[22] P. Lu, J. Lai, D. Ma, G. Hsiue, Carbodiimide cross-linked hyaluronic acid hydrogels as cell sheet delivery vehicles: characterization and interaction with corneal endothelial cells, J. Biomat. Sci. Polym. E 19 (2008) 1–18.
[23] S. Khetan, et al., Degradation-mediated cellular traction directs stem cell fate in covalently crosslinked three-dimensional hydrogels, Nat. Mater. 12 (2013) 458.
[24] C.M. Nimmo, S.C. Owen, M.S. Shoichet, Diels-Alder Click cross-linked hyaluronic acid hydrogels for tissue engineering, Biomacromolecules 12 (2011) 824–830.
[25] D. Xing, L. Ma, C. Gao, A bioactive hyaluronic acid–based hydrogel cross-linked by Diels–Alder reaction for promoting neurite outgrowth of PC12 cells, J. Bioact. Compat. Pol. 244 (2017) 81–128.
[26] V. Crescenzi, L. Cornelio, C. Di Meo, S. Nardecchia, R. Lamanna, Novel hydrogels via click Chemistry: synthesis and potential biomedical applications, Biomacromolecules 8 (2007) 1844–1850.
[27] N. Broguiere, L. Isenmann, M. Zenobi-Wong, Novel enzymatically cross-linked hyaluronan hydrogels support the formation of 3D neuronal networks, Biomaterials 99 (2016) 47–55.
[28] D.B. Dr, S. Mohnani, A. Llanes-Pallas, Supramolecular Chemistry at interfaces: molecular recognition on nanopatterned porous surfaces, Chem. Eur. J. 15 (2009) 7004–7025.
[29] X. He, B. Wei, Y. Mi, Aptamer based reversible DNA induced hydrogel system for molecular recognition and separation, Chem. Commun. 46 (2010) 6308–6310.
[30] W. Li, et al., Multifunctional nanoparticles via host-guest interactions: a universal platform for targeted imaging and light-regulated gene delivery, Chem. Commun. 50 (2014) 1579–1581.
[31] A. Harada, R. Kobayashi, Y. Takashima, A. Hashidzume, H. Yamaguchi, Macroscopic self-assembly through molecular recognition, Nat. Chem. 3 (2011) 34–37.
[32] K.M. Park, et al., In situ supramolecular assembly and modular modification of hyaluronic acid hydrogels for 3D cellular engineering, Acs Nano 6 (2012) 2960–2968.
[33] M.S. Thompson, et al., Self-assembling hydrogels crosslinked solely by receptor-ligand interactions: tunability, rationalization of physical properties, and 3D cell culture, Chem. Eur. J. 21 (2015) 3178–3182.
[34] A. Breen, T. O'Brien, A. Pandit, Fibrin as a delivery system for therapeutic drugs and biomolecules, Tissue Eng. Part B Rev. 15 (2009) 201–214.
[35] R.I. Litvinov, O.V. Gorkun, S.F. Owen, H. Shuman, J.W. Weisel, Polymerization of fibrin: specificity, strength, and stability of knob-hole interactions studied at the single-molecule level, Blood 106 (2005) 2944–2951.
[36] A.S. Soon, S.E. Stabenfeldt, W.E. Brown, T.H. Barker, Engineering fibrin matrices: the engagement of polymerization pockets through fibrin knob technology for the delivery and retention of therapeutic proteins, Biomaterials 31 (2010) 1944–1954.
[37] L.P.P. De, D. Ludeña, Cell culture in autologous fibrin scaffolds for applications in tissue engineering, Exp. Cell Res. 322 (2014) 1–11.
[38] N. Laurens, P. Koolwijk, M.P. de Maat, Fibrin structure and wound healing, J. Thromb. Haemost. 4 (2006) 932–939.
[39] L. Bian, et al., The influence of hyaluronic acid hydrogel crosslinking density and macromolecular diffusivity on human MSC chondrogenesis and hypertrophy, Biomaterials 34 (2013) 413–421.
[40] C.G. Williams, A.N. Malik, T.K. Kim, P.N. Manson, J.H. Elisseeff, Variable cytocompatibility of six lines with photoinitiators used for polymerizing hydrogels and cell encapsulation, Biomaterials 26 (2005) 1211–1218.
[41] S.J. Bryant, C.R. Nuttelman, K.S. Anseth, Cytocompatibility of UV and visible light photoinitiating systems on cultured NIH/3T3 fibroblasts in vitro, J. Biomat. Sci. Polym. E Polym. Ed. 11 (2000) 439–457.